Synthesis and Design of Dual-Wideband Bandpass Filters With Internally-Coupled Microstrip Lines

Runqi Zhang [1] and Lei Zhu [2]
[1] School of Electrical and Electronic Engineering, Nanyang Technological University, Singapore
[2] Faculty of Science and Technology, University of Macau, Macau SAR, China
Emails: rzhang1@e.ntu.edu.sg, leizhu@umac.mo

Abstract—A class of dual-wideband bandpass filters (BPFs) with internally-coupled microstrip lines has been proposed and exactly synthesized in this paper. The generic structure of the proposed filters is formed by folding a multi-mode resonator (MMR) along its symmetrical plane and coupling a pair of short-circuited stubs on the two ends of the MMR. Thus, two coupling paths, one from the folded MMR and another from the coupled stubs, are used to generate additional transmission zeros (TZs) between the two passbands. A general synthesis procedure is developed for the synthesis of these BPFs by matching the transfer function of the circuit to the prescribed filtering function. As a design example, a 1st order BPF is firstly formed by using the coupled short-circuited stubs to illustrate the tunable distribution of the two reflection zeros. Secondly, a 2nd order dual-band BPF is designed with fully internally-coupled microstrip lines to provide an extra degree of freedom in determination of the design parameters. Next, a 3rd order BPF is partially coupled to have an explicit expression of the generated TZs. Finally, a 2nd-, 3rd-order and a cascaded case are synthesized and designed. The experimental results agree closely with the synthesized and designed ones.

I. INTRODUCTION

Microstrip bandpass filters (BPFs) have been extensively studied and developed for a long time to meet various requirements in many modern communication systems. Among these designs, planar types of narrow and wide dual-band BPFs are highly promising in size compactness, large out-of-band rejection, low fabrication cost, and etc. [1]-[14].

Many design methods for dual-narrowband BPFs have been reported [1]-[8]. In [1], two narrowband BPFs of different center frequencies are parallel-connected and fed by dual-band impedance matching networks. Stepped-impedance resonators (SIRs) are used to apply the fundamental- and its higher-order resonances to form the first and second passbands, as reported in [2]-[3]. To reduce the overall size of the circuit, single ring/patch resonators have also been used to form a class of dual-mode dual-band BPFs in [4]-[6]. But, most of these designs are involved with a complicated design process or based on a cut-and-try method. Furthermore, due to the approximate condition assumed in the filter design process, they are strictly limited to dual-narrowband filter designs. Some frequency transformation techniques have been proposed in [7]-[8] to solve this problem to a certain degree. A successive frequency transformation method has been proposed in [7] to transfer a lowpass circuit prototype to its single- and dual-band bandpass counterparts. In [8], a single-band resonator is readily transferred to a multi-band network. Based on this transformation, a corresponding filtering structure and its frequency response are derived. However, most of the frequency transformation methods are established using the frequency-invariant *J*/*K* transformers, thus restraining their usage for most wideband BPFs.

Due to the difficulties discussed above, only a few dual- wideband BPFs have been reported so far [9]-[14]. Using the technique in [1], a dual-wideband BPF [9] is designed by connecting two wideband BPFs in parallel and mounting dual-band matching networks in external feed lines. Another class of dual-wideband BPFs can be realized by connecting a bandstop filter (BSF) with a wideband BPF [10] or embedding the BSF into a wide BPF [11]. However, for these dual-wideband BPFs, a synthesis methodology has rarely been developed so far to meet the predefined specifications.

In [12]-[14], a concept of signal interaction has been proposed by forming a loop-shaped circuit for design of an

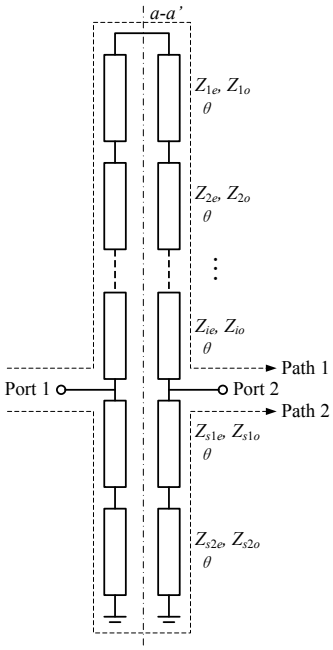

Fig. 1. General schematic of the proposed dual-wideband BPF with internally-coupled microstrip lines.

alternative class of dual-band BPFs. In [12], two transmission lines of 180° difference in phase are parallel-connected so as to generate new pairs of transmission zeros (TZs) between the two desired passbands. In [13], a dual-band BPF is formed by introducing additional open-stubs on the loop circuits. However, these two designs cannot effectively block the DC component. Another type of dual-band BPF is formed by parallel-connecting two wideband BPFs to create an additional pair of TZs within the two passbands [14]. Though a complete synthesis procedure is developed, the order of each filter block has to be fixed at a certain integer. Except the above mentioned frequency symmetry cases, a synthesis method for asymmetry frequency response is presented in [15], and a practical case is realized by stepped-impedance lines to individually adjust the bandwidth of the two passbands [16].

In this paper, a class of dual-wideband BPFs with internally-coupled microstrip lines have been proposed, synthesized and designed. First, a multi-mode resonator (MMR) is symmetrically folded to form up the internally-coupled microstrip lines. By adding more sections of the coupled MMR, the order of the proposed filter is increased. Then, a pair of short-circuited stubs is introduced to inductively couple with the MMR. By further introducing a mutual coupling between the two short-circuited stubs, another coupling path is formed to generate additional pairs of TZs at either the real or imaginary frequencies. The synthesis procedure for the proposed BPFs mainly includes three steps: (a) deriving the theoretical filtering function, (b) analyzing the chosen circuit response based on its transfer function, and (c) obtaining the circuit design parameters with equating the two aforementioned functions. Filter prototypes of order 2^{nd}-3^{rd} as well as a cascaded dual-band filter are synthesized and designed. Compared with the previous work in [14], the proposed dual-band BPFs have much more flexibility in controlling the filter order of each unite block, permitting an extra degree of freedom in choosing appropriate impedance values and also promising to realize a compact circuit size when a fully internally-coupled structure is used.

II. Design and Synthesis Procedure

The synthesis technique used herein shares a similar design procedure and generic transfer function as discussed in [14]. However, the circuit structure is an alternative improvement compared with the ones of [14] in the following aspects:

a) The order of every single filtering block: this work has a capability of varying from 1-3 (seen Table I) while that in [14] being fixed at 3;

TABLE I

STRUCTURES OF THE PROPOSED DUAL-BAND BPF PROTOTYPES

Filter Structure	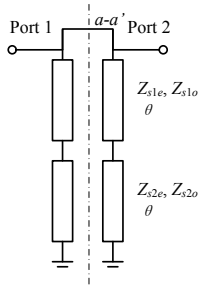	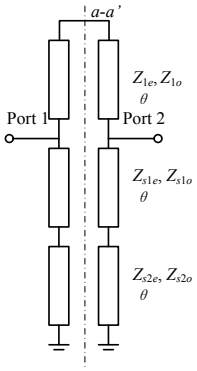	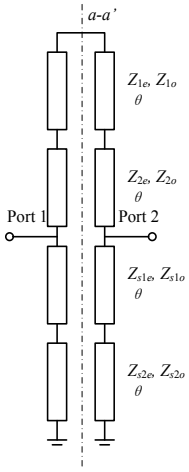
n	1	2	3
$\begin{Bmatrix} Y_{ine}, \\ Y_{ino} \end{Bmatrix}$	$\begin{Bmatrix} \dfrac{k_1 + k_2 t^2}{k_3 t}, \\ \infty \end{Bmatrix}$	$\begin{Bmatrix} \dfrac{k_1 + k_2 t^2}{k_3 t}, \\ \dfrac{k_4 + k_5 t^2}{k_6 t} \end{Bmatrix}$	$\begin{Bmatrix} \dfrac{k_1 + k_2 t^2 + k_3 t^4}{k_4 t + k_5 t^3}, \\ \dfrac{k_6 + k_7 t^2}{k_8 t} \end{Bmatrix}$
F_{cir}	$\dfrac{\begin{bmatrix} -k_1 \\ -k_2 t^2 \end{bmatrix}}{Y_0 t k_3}$	$\dfrac{\begin{bmatrix} -k_1 k_4 \\ \left(Y_0^2 k_3 k_6 - k_2 k_4 - k_1 k_5\right) t^2 \\ -k_2 k_5 t^4 \end{bmatrix}}{Y_0 t \begin{bmatrix} \left(k_4 k_3 - k_1 k_6\right) \\ \left(k_5 k_3 - k_2 k_6\right) t^2 \end{bmatrix}}$	$\dfrac{\begin{bmatrix} -k_1 k_6 \\ \left(Y_0^2 k_8 k_4 - k_1 k_7 - k_6 k_2\right) t^2 \\ \left(Y_0^2 k_8 k_5 - k_2 k_7 - k_3 k_6\right) t^4 \\ -k_3 k_7 t^6 \end{bmatrix}}{Y_0 t \begin{bmatrix} \left(k_6 k_4 - k_8 k_1\right) \\ \left(k_7 k_4 + k_6 k_5 - k_8 k_2\right) t^2 \\ \left(k_7 k_5 - k_8 k_3\right) t^4 \end{bmatrix}}$

where t=tan(θ), n is the order of each individual band of the dual-band bandpass filter, Y_{ine} and Y_{ino} the input admittance of the even- and odd-mode circuit, respectively, F_{cir} the transfer function of the filter and k_i (i=1, 2,…) represents the coefficients of the polynomial formed by the impedance of the coupled line.

b) The characteristic impedance: this work produces an extra degree of freedom in choosing appropriate impedance values for fabrication (seen Section III.B) while that in [14] being fixed;
c) The circuit size: this work benefits from size reduction thanks to the coupled structure while that in [14] being much larger in overall size than that presented in this work.

A. Circuit Analysis of the Proposed Dual-Band Filters

The generic structure of the proposed dual-band BPF is depicted in Fig. 1, in which Z_{ie} and Z_{io} (i= 1, 2, …) denote the even- and odd-impedances of the i-th coupled-line section in the folded MMR (internally-coupled), while (Z_{s1e}, Z_{s2e}) and (Z_{s1o}, Z_{s2o}) represent the even- and odd-impedances of the two coupled short-circuited stubs (parallel coupled), respectively. To simplify the synthesis process, it is assumed that for all the coupled-line sections involved, their electrical lengths are set as the same, $\theta_e = \theta_o = \theta$, regardless of even- or odd-mode excitations, where θ is defined at the middle frequency of the two passbands.

For the MMR with the 2i line sections in Fig.1, it is to introduce (2i-1) reflection zeros within the interested passbands. By applying this property in a filter design, increasing the section number of the MMR leads to more reflection zeros within the passband, as discussed in [17]. When the MMR is folded along its symmetrical plane as shown in Fig. 1, the design parameter is split from the characteristic impedance, Z_i, of an uncoupled line to the even-

and odd-impedances, Z_{ie} and Z_{io}, of the coupled lines, releasing twice design parameters compared with the un-coupled MMR. Therefore, it permits an extra degree of freedom in determining these impedance parameters during the filter design process. According to the study in [18], the folded MMR modifies or reshapes the phase distribution of current density flowing along its two sides, providing a great potential in creating more pairs of TZs at specified frequencies.

As studied in [17], the two short-circuited stubs will be used herein to inductively feed or excite the folded MMR at its two sides, and they also introduce more reflection zeros in the passbands. In the meantime, these two coupled stubs provide another coupling path beside the coupled MMR. With these two paths, additional reflection zeros are generated.

First, the theoretical analysis of the proposed dual-band BPF in Fig. 1 is carried out by applying the even- and odd-mode method with respect to the symmetrical plane of *a-a'*. The transfer function F_{cir} is obtained as [19]

$$F_{cir} = \frac{S_{11}}{S_{21}} = \frac{Y_0^{\,2} - Y_{ine}Y_{ino}}{Y_0\left(Y_{ino} - Y_{ine}\right)} \tag{1}$$

where, Y_0 stands for the port admittance, Y_{ine} and Y_{ino} are the input admittances of the one-port even- and odd-symmetrical bisection circuits, respectively. Table I depicts the structures of the first three filter prototypes with the 1st, 2nd and 3rd order, and it provides the derived mathematical expressions for the input admittances of the three one-port even- and odd-mode bisections as well as transfer functions of the three two-port filter circuits to be synthesized.

In (1), the numerator of F_{cir} indicates the number and positions of the reflection zeros, and it is in the form of an even order polynomial as a function of t (t= tan(θ)). Therefore, the reflection zeros are distributed in pairs with mirror to $\theta = \pi/2$. Meanwhile, the denominator of F_{cir} implies the number and positions of the TZs, and it is in the form of an even order polynomial multiplied by t. Thus, there always exists a TZ at $\theta = 0$ and π, and the rest ones are paired with mirror to $\theta = \pi/2$. It is found that the polynomial of the numerator is always one degree higher than that of the denominator. As t approaches infinity, F_{cir} becomes infinite, indicating that a TZ is located at $\theta = \pi/2$. Based on the above discussions, the TZs at $\theta = 0$, $\pi/2$ and π shaping the basic filtering response of the dual-band BPF, and the reflection zeros locate symmetrically with respect to $\theta = \pi/2$ forming the dual-passband.

B. Dual-Band Theoretical Filtering Function

As for the synthesis, a generalized Chebyshev filtering function is established based on a transversal coupling scheme, taking into account of the TZ at origin, instead of the commonly used ones in [20] for the narrow dual-band BPFs. The nth-order filtering function as a function of Ω is given as [21]

$$F_n\left(\Omega\right) = \cosh\left(\cosh^{-1}\left(\frac{T_2(\Omega)}{|\Omega|}\right) + \sum_{k=1}^{n-1}\cosh^{-1}\left(f_k\left(\Omega\right)\right)\right) \tag{2a}$$

where $f_k\left(\Omega\right) = \left[T_1\left(\Omega\right) - \frac{1}{T_1\left(z_k\right)}\right] \Big/ \left[1 - \frac{T_1\left(\Omega\right)}{T_1\left(z_k\right)}\right]$,

$$T_1(\Omega) = \frac{1}{\Omega_2^{\,2} - \Omega_1^{\,2}}\left[2\Omega^2 - \left(\Omega_1^{\,2} + \Omega_2^{\,2}\right)\right],$$

$$T_2(\Omega) = \frac{1}{\Omega_2 - \Omega_1}\left(\Omega^2 - \Omega_1\Omega_2\right) \tag{2b}$$

in which Ω_1 and Ω_2 refers to the lower and upper edge frequencies of the filtering function, respectively, and z_k is the location of the TZ. Next, a recursion formula [21] is derived to expand the filtering function to a ratio of two polynomials.

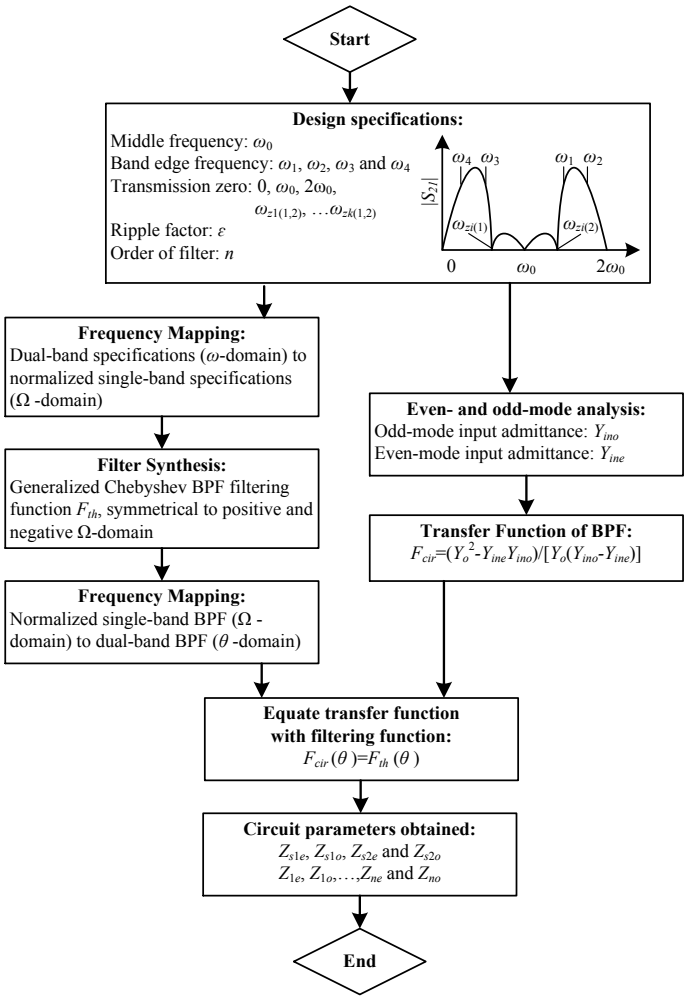

Fig. 2. Synthesis procedure for the proposed dual-band BPFs.

C. Synthesis of the Proposed Dual-Band BPFs

The synthesis procedure for the proposed dual-wideband BPF is illustrated in Fig. 2, i.e., (a) formulating the filtering function, (b) analyzing the frequency response of the filter circuit, and (c) enforcing the equalization of these two functions so as to determine all the circuit design parameters, as documented in [22]. Since the generalized Chebyshev transfer function to be chosen is only valid for a single band modeling with mirror to the origin, a frequency mapping, namely, Richards transform [23], is used to transfer the single-band function to its dual-band counterpart. Accordingly, the transformation from the ω-domain to the Ω-domain [20] can be derived in the form of

$$\Omega = -\delta / \tan\theta, \quad \theta = \frac{\pi}{2}\frac{\omega}{\omega_0} \tag{3}$$

$$\delta = 1/\tan\left[\frac{\pi}{4}\frac{(\omega_2-\omega_4)}{\omega_0}\right] \tag{4}$$

where ω_2 and ω_4 are the upper and lower edge frequencies of the dual-band BPF, respectively, with reference to Fig. 2.

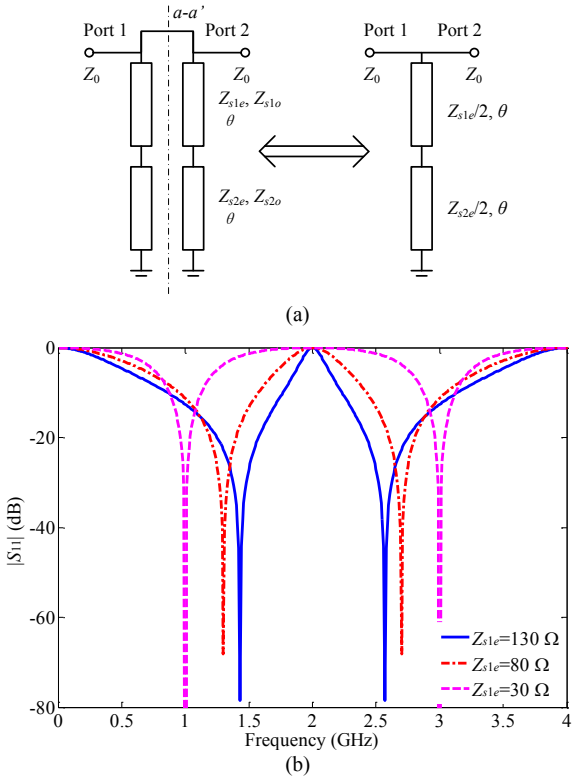

Fig. 3. (a) Transmission-line characterization of the parallel-coupled short-circuited stubs and its equivalent circuit of the stepped-impedance stub. (b) Locations of the reflection zeros under different impedance value of Z_{s1e} (Z_{s2e}= 30 Ω).

Once the specifications of the filter are prescribed, these ω-domain frequencies are transferred to the Ω-domain for building up the filtering function. Afterwards, the filtering function is transferred back to the θ-domain in order to exactly match the transfer function of the circuit in the form of

$$\varepsilon F_n(\Omega)\Big|_{\Omega=-\frac{\delta}{\tan\theta}} = jF_{cir}(\tan\theta) \tag{5}$$

where ε is the in-band ripple factor for the dual passbands. A set of non-linear equations is obtained by setting the coefficients of the numerator and the denominator between the two functions to be equal, respectively. An iterative/optimization method [24] is applied herein to solve these nonlinear equations, with the initial value chosen from the two parallel-connected UWB filters of similar bandwidth of $(\theta_2$-$\theta_4)/90^o$. However, it is noted that the proposed synthesis procedure is theoretically applicable to a broad range of specifications limited by the practically realizable coupled impedance values.

III. Synthesis and Design of Dual-Band BPFs

A. 1st Order Dual-Band BPF Design

First, a special case formed by two coupled short-circuited stubs is discussed. Under odd-mode excitation, the circuit is virtually shorted to ground. While under even-mode excitation, its bisection circuit contributes to the frequency response in the desired passband. Therefore, the coefficient of the transfer function F_{cir} is only related to its even-mode impedances as

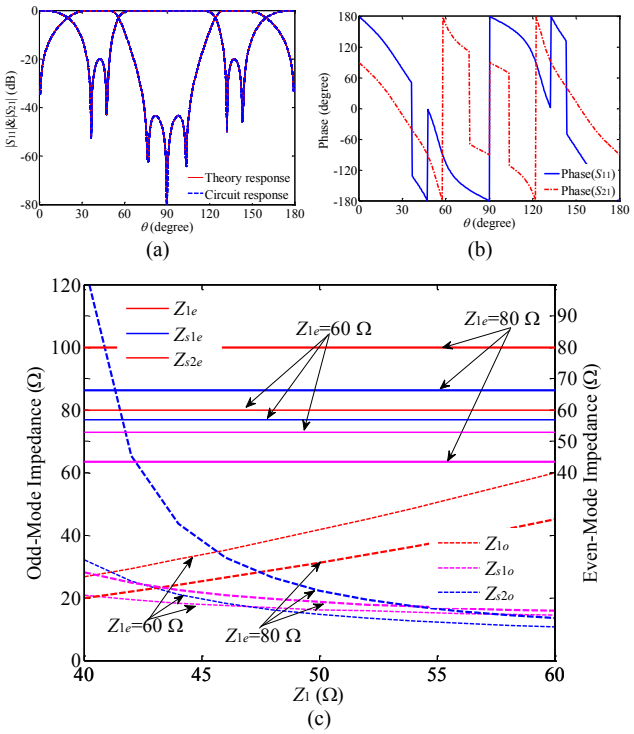

Fig. 4. (a) Comparison between theoretical and circuit magnitude responses of a 2nd order filter under the targeted specifications: ε=0.1, θ_{tz2}= 76.5°, θ_1= 123.75° and θ_2= 139.5°. (b) Phase responses. (c) Impedance values versus Z_{1e} and Z_1 for determining the responses (magnitude and phase) in Fig. 3(a)-(b).

$$\begin{cases} k_1 = Z_{1se} \\ k_2 = -Z_{2se} \\ k_3 = jZ_{1se}\left(Z_{2se} + Z_{1se}\right) \end{cases} \tag{6}$$

Actually, the parallel-coupled short-circuited stubs could be further simplified as a two-section stepped-impedance stub, as shown in Fig. 3(a). Besides the TZs (θ_{tz1}) at multiple integer of $\pi/2$, there is also one pair of reflection zeros with mirror to the middle frequency of the two passbands. As the impedance ratio of the stepped-impedance stubs changes, the frequency ratio of the two reflection zeros varies accordingly [25], as illustrated in Fig. 3(b). Based on the above discussion, the short-circuited stubs has two main roles for the proposed filter design, first, introducing TZs to shape dual-band frequency-response, second, introducing one pair of tunable reflection zeros at the desired positions within each band

B. 2nd Order Dual-Band BPF Design

To increase the filter order for sharp rejection slope, one more section is added in the coupled MMR, as tabulated in Table I. According to the even-odd mode analysis, the transfer function of this 2nd order dual-band filter is derived, with its definition of the coefficients (k_1-k_6) as

$$\begin{cases} k_1 = Z_{1e}Z_{s1e} \\ k_2 = -\left(Z_{s1e}Z_{s2e} + Z_{s1e}Z_{s1e} + Z_{1e}Z_{s2e}\right) \\ k_3 = jZ_{1e}Z_{s1e}\left(Z_{s2e} + Z_{s1e}\right) \\ k_4 = j\left(Z_{s1o}Z_{s2o} + Z_{s1o}Z_{s1o} + Z_{1o}Z_{s1o}\right) \\ k_5 = -jZ_{1o}Z_{s2o} \\ k_6 = -Z_{1o}Z_{s1o}\left(Z_{s2o} + Z_{s1o}\right) \end{cases} \tag{7}$$

Besides the TZs located at $\theta_{tz1}= 0$, $\pi/2$ and π, there is one pair of TZs at θ_{tz2}, and they could be explicitly expressed as

$$\begin{cases} \tan\theta_{tz1} = 0,\ \infty \\ \tan\theta_{tz2} = \pm\sqrt{\dfrac{(k_1k_6 - k_4k_3)}{(k_5k_3 - k_2k_6)}} \end{cases} \tag{8}$$

From the derived transfer function in Table I, there are 3 and 2 coefficients for its numerator and denominator, respectively. These unknown coefficients are expressed in the form of impedance values of the circuit. First, the highest order of either the numerator or denominator is normalized, so that the number of the unknown coefficients can be reduced to only 4. Next, for the internally-coupled dual-band BPF, there are 6 impedance parameters (Z_{1e}, Z_{1o}, Z_{s1e}, Z_{s1o}, Z_{s2e}, and Z_{s2o}) to be solved. So, the 4 unknown coefficients are overly determined by the 6 circuit parameters. In other words, it is possible to have different sets of impedance parameters to get the same sets of polynomial coefficients in the transfer function, and to obtain the same filtering responses in the end. Therefore, there exists an extra degree of freedom when determining the impedance values. Following this design strategy, 2 of the 6 parameters are predefined at certain values as a design example to illustrate the flexibility in controlling the impedance parameters synthesized. These two design variables are the impedance values of the MMR (Z_{1e} and Z_{1o}) and they are selected under the criteria of $Z_1 = \sqrt{Z_{1e}Z_{1o}}$. Under different choices of Z_{1e} and Z_{1o}, different solutions of Z_{s1e}, Z_{s1o}, Z_{s2e}, and Z_{s2o} are obtained while maintaining the same frequency response.

Fig. 4(a) plots the typical simulated frequency response of a 2nd order dual-band BPF using the theoretical filtering function and synthesized circuit transfer function, respectively. Both sets of frequency responses are indistinguishable to each other, so it well verifies the proposed synthesis method. Fig. 4(b) depicts the phase variations in relevance to the circuit responses, and Fig. 4(c) presents different sets of impedance solutions to give the same magnitude and phase responses as those in Fig. 4(a)-(b). Therefore, it also proves the proposed technique on extra degree of freedom in choosing different sets of impedance values.

Further looking into Fig. 4(c), once Z_{1e} is chosen as either 60 or 80 Ω, the even-mode impedances, Z_{1e}, Z_{s1e} and Z_{s2e}, can be fixed as certain values. A set of straight lines is used to characterize the variation of the even-mode impedance value. As Z_1 is swept, Z_{1o} is changed, as $Z_{1o}= Z_1^2/ Z_{1e}$, and it causes the variation of the odd-mode impedance values. Therefore, a set of curves is used for their variation. This regulation can be simply verified by the characteristics of the even/odd mode analysis, namely, the even-mode bisection circuit being unrelated to its odd-mode counterpart. Therefore, it is possible to get a set of even- and odd-mode impedance values respectively to maintain the frequency response of the corresponding even- and odd-mode bisection circuit, and then the frequency response of the whole circuit keeps the same. This provides a foundation to the proposed BPFs in achieving the extra design freedom of the design parameters while maintaining the exactly same frequency response. With this technique, it is advantageous in choosing a set of preferred impedance values suitable the design procedure and/or fabrication.

C. 3rd Order Dual-Band BPF Design

To further increase the order of the filter, the number of the coupled section of the MMR is set as 2, as shown in the schematic in Table I. As the order increases, more design parameters are involved, implying complicated and time-consuming analysis for the solution of these non-linear equations. To simplify our analysis herein, a special case is studied with only one section of internally-coupled line involved ($Z_{s2e} > Z_{s2o}$). Meanwhile, all the remaining ones are set to be uncoupled ones ($Z_{1e}= Z_{1o}= Z_1$, $Z_{2e}= Z_{2o}= Z_2$ and $Z_{s1e}= Z_{s1o}= Z_{s1}$). The coefficients of the polynomials (k_1-k_6) can be accordingly expressed as below,

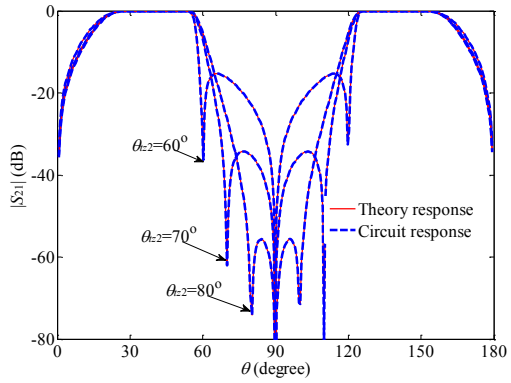

(a)

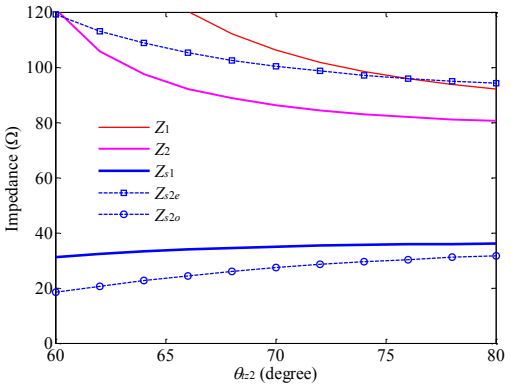

(b)

Fig. 5. (a) Theoretical and circuit responses of a 3rd order filter under the targeted specifications: ε=0.1, θ_1= 117° and θ_2= 144°. (b) Impedance values versus different locations of the TZs (θ_{tz2}).

$$\begin{cases} k_1 = Z_2 Z_{s1} Z_1 \\ k_2 = -\begin{pmatrix} Z_{s1} Z_2 Z_{s2e} + Z_{s1} Z_1 Z_{s2e} + Z_{s1} Z_2 Z_{s1} \\ + Z_{s1} Z_1 Z_{s1} + Z_2 Z_{s1} Z_2 + Z_2 Z_1 Z_{s2e} \end{pmatrix} \\ k_3 = Z_2 Z_2 Z_{s2e} \\ k_4 = jZ_{s1} Z_2 Z_1 \left(Z_{s2e} + Z_{s1} \right) \\ k_5 = -jZ_{s1} Z_2 Z_2 \left(Z_{s2e} + Z_{s1} \right) \\ k_6 = jZ_2 Z_{s1} \left(Z_{s2o} + Z_{s1} + Z_1 + Z_2 \right) \\ k_7 = -\left[jZ_2 \left(Z_1 + Z_2 \right) Z_{s2o} + jZ_{s1} \left(Z_{s2o} + Z_{s1} \right) Z_1 \right] \\ k_8 = -Z_2 Z_{s1} \left(Z_1 + Z_2 \right) \left(Z_{s2o} + Z_{s1} \right) \end{cases} \tag{9}$$

In this way, the 5 impedance design parameters, namely, Z_1, Z_2, Z_{s1}, Z_{s2e} and Z_{s2o}, are exactly matched to the 5 unknown coefficients in the numerator and normalized denominator of a filtering function. Though this arrangement lacks the freedom in choosing the preferred impedance values, it leads to explicit expressions of the TZs in the form of

$$\begin{cases} \tan\theta_{tz1} = 0,\ \infty \\ \tan\theta_{tz2} = \pm\sqrt{\dfrac{\left(k_7 k_5 - k_8 k_3 \right)}{\left(k_8 k_1 - k_6 k_4 \right)}} \\ \tan\theta_{tz3} = \pm j \end{cases} \tag{10}$$

Similar to the design of the 2nd order filter in the previous section, θ_{tz1} introduces TZs at multiple integer of $\pi/2$ for a periodic property of the tan(θ) function. The paired TZs (θ_{tz2}) can be properly allocated in between the two

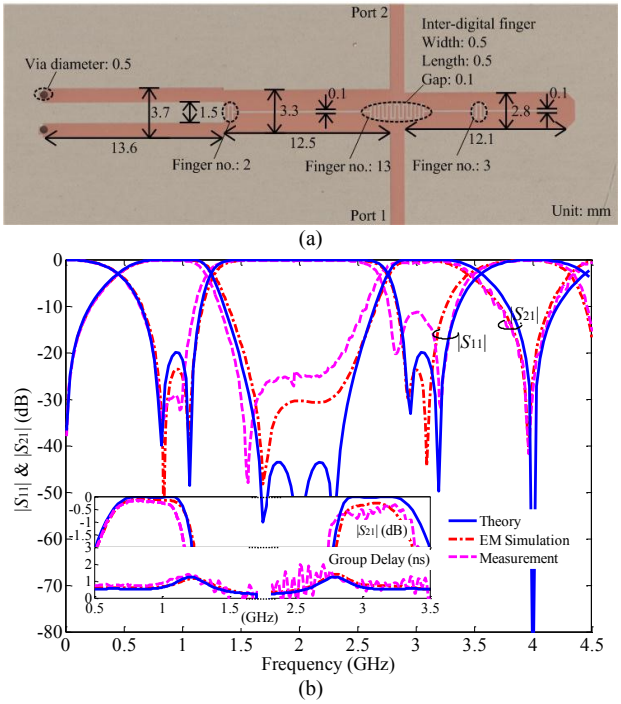

Fig. 6. (a) Photograph of the fabricated 2nd order dual-band filter with dimensions labeled. (b) Comparison between the theoretical, EM simulated and measured results of the dual-band filter.

passbands so as to improve the out-of-band rejection performance in the middle stopband. Besides them, there is one more pair of TZs (θ_{tz3}) fixed at two constant imaginary frequencies.

Fig. 5(a) depicts the frequency responses under different locations of the predefined TZs. As the paired TZs move to the middle of the two passbands, the rejection in this stopband gets great enhancement, whereas the roll-off skirt near the edge of the dual passbands deteriorates gradually, and vice versa. Fig. 5(b) shows the variations of the three impedances with respect to the location of the TZs. To further improve the out-of-band rejection, the proposed dual-band BPFs can be folded in close proximity to introduce the cross coupling between the input and output ports, as discussed in [6].

IV. Experimental Results and Discussions

In this section, the 2nd and 3rd order dual-band BPFs as well as a higher order dual-band BPF with two kinds of filter blocks cascaded are implemented, fabricated and discussed. The substrate used has a dielectric constant of 10.8, loss tangent of 0.0023, thickness of 50 mils and copper thickness of 0.017 mm. A Commercial EM simulator [26] is applied to get the EM simulation for the microstrip layout.

A. 2nd Order Dual-Band BPF

The circuit specifications of the 2nd order filter are set as, middle frequency of the two passbands at $\omega_0 = 2\pi\times2\times10^9$ rad/s, $\theta_{tz2} = 76.5^o$, $\theta_1 = 123.75^o$, $\theta_2 = 139.5^o$ and the ripple factor $\varepsilon = 0.1$. According to the synthesis design procedure discussed above, the filtering function is obtained as

$$F_2(t) = \frac{141.50t^4 - 249.13t^2 + 94.32}{t^3 - 17.35t} \tag{11}$$

The circuit design parameters are obtained as, $Z_{1e} = 60.0\ \Omega$, $Z_{1o} = 24.0\ \Omega$, $Z_{s1e} = 52.9\ \Omega$, $Z_{s1o} = 22.7\ \Omega$, $Z_{s2e} = 56.8\ \Omega$ and $Z_{s2o} = 44.5\ \Omega$. Due to the approximate assumption of equal even- and odd-mode phase velocity in the

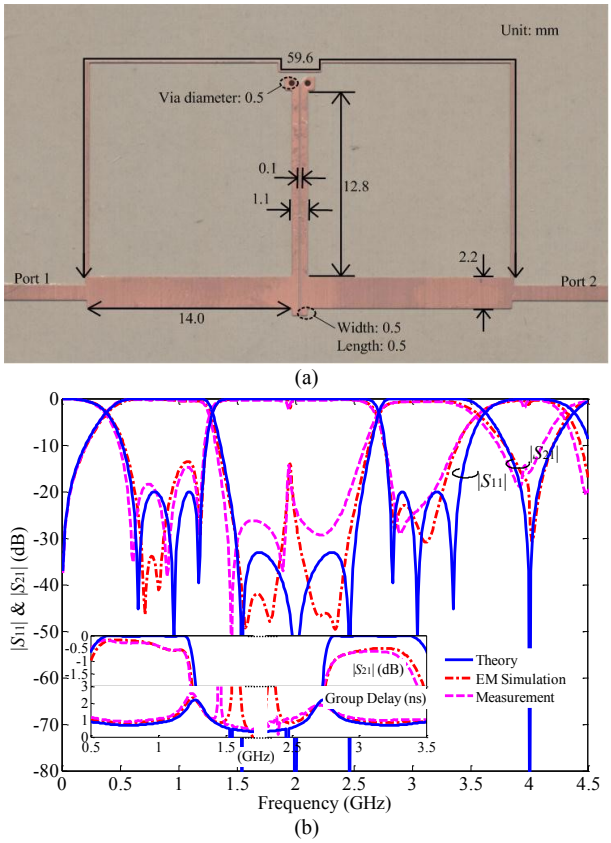

Fig. 7. (a) Photograph of the fabricated 3rd order dual-band filter with dimensions labeled. (b) Comparison between the theoretical, EM simulated and measured results of the dual-band filter.

synthesis design, a compensation method [27]-[28] is utilized herein by adding a capacitor or capacitive element at the two ends of the coupled lines, and an inter-digital capacitor structure is used to realize the required admittance as studied in [29]. The photograph of the fabricated filter is shown in Fig. 6(a). In Fig. 6(b), all the three sets of results from the theory, EM simulation and measurement are in good agreement with each other. The measured results show that for the first/second passband, the center frequency (f_{01}/f_{02}) is 1.03/2.85 GHz, the 3-dB fractional bandwidth (FBW) is 94.8/35.8%, and the insertion loss (IL) is 0.65/0.45 dB, respectively.

B. 3rd Order Dual-Band BPF

The circuit specifications of the 3rd order filter are set as, $\omega_0 = 2\pi\times2\times10^9$ rad/s, $\theta_{tz2} = 69.3^\circ$, $\theta_1 = 117^\circ$, $\theta_2 = 144^\circ$ and $\varepsilon = 0.1$. The filtering function is obtained as

$$F_3(t) = \frac{-81.14t^6 + 237.93t^4 - 191.01t^2 + 39.30}{t^5 - 6.00t^3 - 7.00t} \tag{12}$$

The circuit design parameters are obtained as $Z_1 = 90.7\ \Omega$, $Z_2 = 60.5\ \Omega$, $Z_{s1} = 62.4\ \Omega$, $Z_{s2e} = 79.9\ \Omega$ and $Z_{s2o} = 112.7\ \Omega$. To compensate for unequal even- and odd-mode phase velocities, a section of extended coupled-stubs is used to realize the weak mutual capacitive coupling, as can be seen in Fig. 7(a).

Fig. 7(b) shows the theoretical, EM simulated and the measured results. The measured results show that f_{01}/f_{02} is 0.83/3.13 GHz, 3-dB FBW 105.9/27.3% and IL 0.60/0.85 dB, for the first/second passband, respectively. The measured results match well with the calculated and simulated ones.

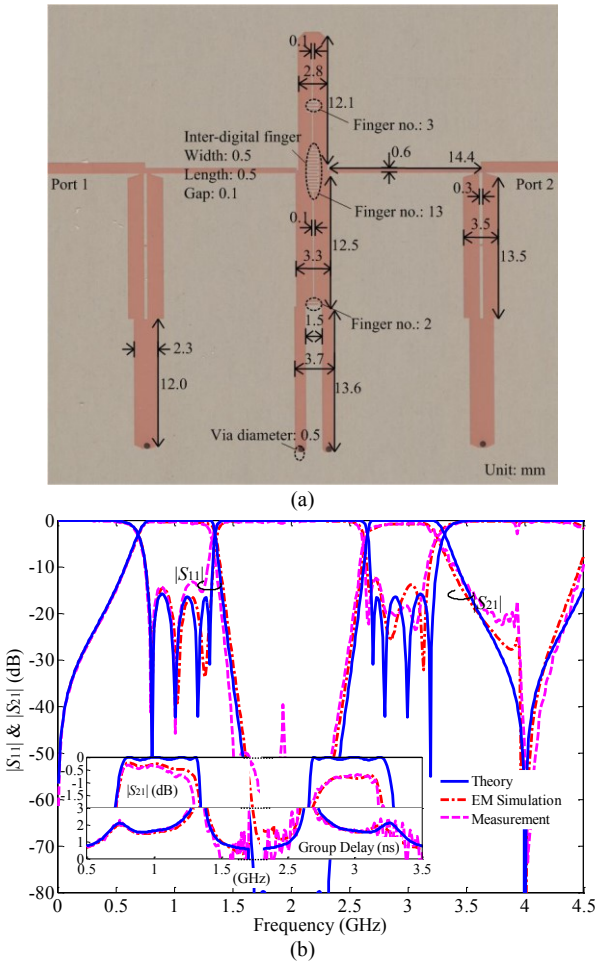

Fig. 8. (a) Photograph of the fabricated cascaded dual-band filter with dimensions labeled. (b) Comparison between the theoretical, EM simulated and measured results of the dual-band filter.

C. 4th Order Dual-Band BPF

A 4th order BPF is formed by cascading two 1st and one 2nd order BPFs, and it is designed to provide one possible method to have a higher order BPF with improved out-of-band rejection. Different from the commonly used design strategy in [12]-[13], the two filter blocks used here are in different orders, serving as an alternative approach. The circuit specifications of this 4th order filter are set as, $\omega_0 = 2\pi\times2\times10^9$ rad/s, $\theta_{tz2} = 76.5^o$, $\theta_1 = 121.0^o$, $\theta_2 = 145.0^o$ and the ripple factor $\varepsilon = 0.15$. The circuit design parameters are, for the 1st order filter block, $Z_{s1e,1} = 60\ \Omega$, $Z_{s1o,1} = 24\ \Omega$ and $Z_{s2} = 33.5\ \Omega$, for the 2nd order filter block, $Z_{1e,2} = 60.0\ \Omega$, $Z_{1o,2} = 24.0\ \Omega$, $Z_{s1e,2} = 52.9\ \Omega$, $Z_{s1o,2} = 22.7\ \Omega$, $Z_{s2e,2} = 56.8\ \Omega$ and $Z_{s2o,2} = 44.5\ \Omega$, and for the line connecting these two blocks, $Z_t = 65.7\ \Omega$. Fig. 8(a) shows the photograph of the fabricated filter. Fig. 8(b) plots the three sets of results from the theory, EM simulation and measurement, and they are found in good agreement with each other. The measured results show that for the first/second passband, f_{01}/f_{02} is 1.03/2.85 GHz, the 3-dB FBW is 94.8/35.8%, and the IL is 0.65/0.45 dB, respectively. For all the three design examples, slight differences between the measured results and theoretical ones are basically caused by several parasitic effects in practical implementation, such as junction discontinuities, dispersion of the microstrip line, and approximate assumption of equal even- and odd-mode phase velocity. The spike in the rejection band may be caused by the phase and magnitude deviation in the two coupling patch.

V. Conclusion

In this paper, a class of dual-wideband BPFs with internally-coupled microstrip lines have been proposed, synthesized and designed. The general structure of the dual-band BPF is formed by a folded MMR and parallel-coupled short-circuited stubs. Due to existence of two dissimilar coupling/signal paths, additional pairs of TZs can be generated in between the two passbands. The synthesis design process follows by theoretically deriving the filtering function, analyzing the circuit response and determining the circuit design parameters under the two equalized functions. As design examples, 1st, 2nd and 3rd order dual-wideband BPFs have been analyzed, discussed and synthesized. In the end, three filter prototypes have been designed, fabricated and measured to verify the proposed design principle in experiment.

References

[1] H. Miyake, S. Kitazawa, T. Ishizaki, T. Yamada and Y. Nagatomi, "A miniaturized monolithic dual band filter using ceramic lamination technique for dual mode portable telephones," in *IEEE MTT-S Int. Dig.*, Jun. 1997, pp. 789-792.

[2] W.-S. Chang and C.-Y. Chang, "Analytical design of microstrip short-circuit terminated stepped-impedance resonator dual-band filters," *IEEE Trans. Microw. Theory Tech.*, vol. 59, no. 7, pp. 1730-1739, Jul. 2011.

[3] S. Sun and L. Zhu, "Compact dual-band microstrip bandpass filter without external feeds," *IEEE Microw. Wireless Compon. Lett.*, vol. 15, no. 10, pp. 644-646, Oct. 2005.

[4] S. Luo, L. Zhu and S. Sun, "Compact dual-mode triple-band bandpass filters using three pairs of degenerate modes in a ring resonator," *IEEE Trans. Microw. Theory Tech.*, vol. 59, no. 5, pp. 1222-1229, May 2011.

[5] Y. C. Chiou, C. Y. Wu and J. T. Kuo, "New miniaturized dual-mode dual-band ring resonator bandpass filter with microwave C-sections," *IEEE Microw. Wireless Compon. Lett.*, vol. 20, no. 2, pp. 67-69, Feb. 2010.

[6] R. Zhang, L. Zhu and S. Luo, "Dual-mode dual-band bandpass filter using a single slotted circular patch resonator," *IEEE Microw. Wireless Compon. Lett.*, vol. 22, no. 5, pp. 233-235, May 2012.

[7] X. Guan, Z. Ma, P. Cai, Y. Kobayashi, T. Anada and G. Hagiwara, "Synthesis of dual-band bandpass filters using successive frequency transformations and circuit conversions," *IEEE Microw. Wireless Compon. Lett.*, vol. 16, no. 3, pp. 110-112, Mar. 2006.

[8] A. García-Lampérez and M. Salazar-Palma, "Single-band to multiband frequency transformation for multiband filters," *IEEE Trans. Microw. Theory Tech.*, vol. 59, no. 12, pp. 3048-3058, Dec. 2011.

[9] S. Oshima, K. Wada, R. Murata and Y. Shimakata, "Multilayer dual-band bandpass filter in low-temperature co-fired ceramic substrate for ultra-wideband applications," *IEEE Trans. Microw. Theory Tech.*, vol. 58, no. 3, pp. 614-623, Mar. 2010.

[10] L.-C. Tsai and C.-W. Hsue, "Dual-band bandpass filters using equal-length coupled-serial-shunted lines and Z-transform technique," *IEEE Trans. Microw. Theory Tech.*, vol. 52, no. 4, pp. 1111-1117, Apr. 2004.

[11] A.-S. Liu, T.-Y. Huang and R.-B. Wu, "A dual wideband filter design using frequency mapping and stepped-impedance resonators," *IEEE Trans. Microw. Theory Tech.*, vol. 56, no. 12, pp. 2921-2929, Dec. 2008.

[12] R. Gómez-García, M. Sánchez-Renedo, B. Jarry, J. Lintignat and B. Barelaud, "A class of microwave transversal signal-interference dual-passband planar filters," *IEEE Microw. Wireless Compon. Lett.*, vol. 19, no. 3, pp.158-160, Mar. 2009.

[13] R. Gómez-Garcia and M. Sánchez-Renedo, "Microwave dual-band bandpass planar filters based on generalized branch-line hybrids," *IEEE Trans. Microw. Theory Tech.*, vol. 58, no. 12, pp. 3760-3769, Dec. 2010.

[14] R. Zhang and L. Zhu, "Synthesis and design of wideband dual-band bandpass filters with controllable in-band ripple factor and dual-band isolation," *IEEE Trans. Microw. Theory Tech.*, to be published.

[15] J. Lee and K. Sarabandi, "A synthesis method for dual-passband microwave filters," *IEEE Trans. Microw. Theory Tech.*, vol. 55, no. 6, pp. 1163-1170, June 2007.

[16] R. Gómez-García, J. Muñoz-Ferreras and M. Sánchez-Renedo, "Signal-interference stepped-impedance-line microstrip filters and application to duplexers," *IEEE Microw. Wireless Compon. Lett.*, vol. 21, no. 8, pp.421-423, Aug. 2011.

[17] R. Zhang and L. Zhu, "Synthesis design of a wideband bandpass filter with inductively coupled short-circuited multi-mode resonator," *IEEE Microw. Wireless Compon. Lett.*, vol. 22, no. 10, pp. 509-511, Oct. 2012.

[18] B. M. Schiffman, "A new class of broad-band microwave 90-Degree phase shifters," *IEEE Trans. Microw. Theory Tech.*, vol. 6, no. 2, pp. 232-237, April. 1958.

[19] I. C. Hunter, *Theory and Design of Microwave Filters*. Institution of Engineering and Technology, 2001, ch. 2 and 5.

[20] J.-Y. Li, C.-H. Chi and C.-Y. Chang, "Synthesis and design of generalized chebyshev wideband hybrid ring based bandpass filters with a controllable transmission zero pair," *IEEE Trans. Microw. Theory Tech.*, vol. 58, no. 12, pp. 3720-3731, Dec. 2010.
[21] S. Amari, F. Seyfert and M. Bekheit, "Theory of coupled resonator microwave bandpass filters of arbitrary bandwidth," *IEEE Trans. Microw. Theory Tech.*, vol. 58, no. 8, pp. 2188-2203, Aug. 2010.
[22] G. C. Temes and J. W. LaPatra, *Introduction to circuit synthesis and design*. New York: McGraw-Hill, 1977.
[23] P. I. Richards, "Resistor-transmission-line circuits," *Proc. IRE*, vol. 36, no. 2, pp. 217- 220, Feb. 1948.
[24] MATLAB Ver. R2010b. Natick, Massachusetts: The MathWorks Inc., 2010.
[25] H.-M. Lee and C.-M. Tsai, "Dual-band filter design with flexible passband frequency and bandwidth selections," *IEEE Trans. Microw. Theory Tech.*, vol. 55, no. 5, pp. 1002-1009, May 2007.
[26] Advanced Design System (ADS). Ver. 2005a, Agilent Technol., Palo Alto, CA, 2005.
[27] S. L. March, "Phase velocity compensation in parallel-coupled microstrip," in *IEEE MTT-S Int. Dig.*, Jun. 1982, pp. 410-412.
[28] D. Michael, "Accurate design of microstrip directional couplers with capacitive compensation," in *IEEE MTT-S Int. Dig.*, May 1990, pp. 581-584.
[29] G. D. Alley, "Interdigital capacitors and their application to lumped-element microwave integrated circuits," *IEEE Trans. Microw. Theory Tech.*, vol. 18, no. 12, pp. 1028- 1033, Dec 1970.